17th World Conference on Earthquake Engineering, 17WCEE
Sendai, Japan - September 13th to 18th 2020

FREQUENCY-DOMAIN STIFFNESS IDENTIFICATION BASED ON ACCELERATIONS ON SPECIFIC FLOORS IN ASYMMETRIC BUILDINGS

K. Nabeshima[(1)]

[(1)] *Assistant Professor, Dept. of Architecture, Faculty of Engineering, Tokyo University of Science, nabeshima.kunihiko@rs.tus.ac.jp*
…

Abstract

Recently, the business continuity plan (BCP) is becoming a leading subject in the world and is being discussed with great concern in the construction and operating process of various built environments. In response to BCP, the structural health monitoring (SHM) has drawn much attention for evaluating the status of buildings and reducing post-earthquake impacts on our society. In developing SHM, the system identification (SI) methodologies, categorized as methods for inverse problems, play a critical role and the modal SI and physical SI are two major well-known branches. The physical SI has the advantage that the stiffness and/or damping coefficients of the structural model can be recovered directly and is well suited to the design of passive control systems. This is also quite useful for the damage detection. Although the physical SI is preferred in SHM, its development is quite limited and slow due to the strict requirement on multiple measurements or the necessity of complicated mathematical manipulation. In particular, investigation on physical SI of three-dimensional (3D) building structures with stiffness or mass eccentricities are more limited.

This paper proposes a new method of frequency-domain physical-parameter system identification of three-dimensional building structures with stiffness eccentricity, which accompany torsional vibration. The two-directional story stiffnesses in the 3D building structure are identified from the horizontal accelerations recoded at the top and first floors. The proposed method has three processes. In the first process, equations of motion in the time domain are transformed into the frequency domain. The theoretical equations to identify the *j*-th two-directional story stiffnesses are derived from the dynamic equilibrium of the free body above the *j*-th story. In the second process, the responses on non-observation floors are evaluated from the horizontal accelerations recoded at the top and first floors with low-order modal shapes. In the last process, all responses are applied to the theoretical equations and the two-directional story stiffnesses are evaluated from the identification result around low-order natural frequency. Compared to the previous approaches, the proposed method has some features and advantages, which are as follows.

- The proposed method is based on Fourier analysis method and avoids complicated mathematical manipulation. Therefore, it provides good usability.
- The two-directional story stiffnesses in the 3D building structure can be identified from the horizontal accelerations recorded at the top and first floors of the building.
- The data with high S/N ratio, which is selected based on low-order modal information, is used for the identification and this makes the proposed method robust for noise.
- The two-directional story stiffnesses for each story can be identified independently. The identification result of one story doesn't affect those of other stories.

The proposed method is demonstrated through numerical simulations. Numerical examples, including the comparison with the numerical simulation results, demonstrated that the proposed method is reliable and possesses an acceptable accuracy. It should be remarked that identification results of story stiffnesses are quite stable around the low-order natural frequency and are robust for noise.

Keywords: physical-parameter identification, torsional response, frequency domain, measurement on specific floors

1. Introduction

Recently, the business continuity plan (BCP) is becoming a leading subject in the world and is being discussed with great concern in the construction and operating process of various built environments. Unprecedented hazards and incidents in the last few decades enhanced BCP to a key subject and many significant efforts on BCP have been devoted to assure the resilience of built environments. In response to BCP, the structural health monitoring (SHM) has drawn much attention for evaluating the status of buildings and reducing post-earthquake impacts on our society.

In developing SHM, the system identification (SI) methodologies, categorized as methods for inverse problems, play a critical role and the modal SI and physical SI are two major well-known branches. Originally, the modal SI as a popular technique was developed extensively. It can provide the overall mechanical properties of a structural system and has a stable characteristic [1-3]. However, the information of high-order mode is required to evaluate damage-degree and damaged location. Furthermore, it is pointed out that the influence of local damage to structural members on modal informations is small [4,5]. On the other hand, the physical SI has the advantage that the stiffness and/or damping coefficients of the structural model can be recovered directly and is well suited to the design of passive control systems. This is also quite useful for the damage detection.

In the physical SI, Nakamura and Yasui [6] proposed a method of direct SI incorporating a least-squares method. They investigated an issue of damage detection for steel building frames which were severely damaged (beam-end fracture etc.) during the Hyogoken-Nanbu (Kobe) earthquake in 1995. Moreover, the method of Takewaki and Nakamura [7] aims at a smart identification and seeks for a unique physical-parameter SI formulation based on the work by Udwadia et al.[8]. They enabled the identification of stiffness and damping at a given story of a shear building model directly from the floor acceleration records just above and below the target story. In the SI method by Takewaki and Nakamura [7,9,10], there remained an issue to be resolved in dealing with actual data, e.g. microtremors, due to the small signal/noise (SN) ratio in the low frequency range (Ikeda et al. [11,12], Fujita et al. [13]). Furthermore, an shear-type building model should be replaced by a more appropriate model when dealing with high-rise buildings with large aspect ratios due to the influence of overall bending deformation of tall buildings. The investigation on shear-bending-type building has been developed extensively [14-17].

The physical SI of 2D building structure (share-type building, shear-bending-type building) has been developed extensively. However, many of the mid- and low-rise building possess stiffness eccentricity due to structural asymmetry and the torsional vibration is induced. Therefore, the physical SI applicable to torsional coupled buildings should be developed extensively in order to estimate structural health more realistically. However, investigation on physical SI of 3D building structures with stiffness eccentricity is quite limited. Recently, Shintani et al. [18] proposed a method physical SI for 3D building structures with in-plane rigid floor diaphram in which the stiffness and damping coefficients of each vertical structural frame in the 3D building structure are recovered from the measured data on floor horizontal accelerations. A method based on the batch processing least-squares estimation was proposed using many discrete time-domain data to directly identify the stiffness and damping coefficients of each vertical structural frame. However, their method has a difficulty that the displacements, velocities, and accelerations on all the floors have to be provided. In addition, the identification accuracy depends on the integration method and the identified values can be unrealistic.

This paper proposes a new method of frequency-domain physical-parameter system identification of three-dimensional building structures with stiffness eccentricity, which accompany torsional vibration. The two-directional story stiffnesses in the 3D building structure are identified from the horizontal accelerations recoded at the top and first floors. The proposed method has three processes. In the first process, equations of motion in the time domain are transformed into the frequency domain. The theoretical equations to identify the j-th two-directional story stiffnesses are derived from the dynamic equilibrium of the free body above the j-th story. In the second process, the responses on non-observation floors are evaluated from the horizontal accelerations recoded at the top and first floors with low-order modal shapes. In the last process, all responses are applied to the theoretical equations and the two-directional story stiffnesses are evaluated from the identification result around low-order natural frequency.

2. Object building model and assumptions

Consider an N-story 3D building model, with stiffness asymmetricity with respect to the x-axis and the y-axis, as shown in Fig.1. The black and white circles shown in Fig.1 denote the centers of stiffness and centers of mass. The frame in the side of the center of stiffness for each axis is called the stiff-side frame and the frame in the other side of the center of stiffness is called the flexible-side frame. L_x, L_y denote the x-directional and y-directional floor sizes. Let $m_j, I_j, e_{xj}, e_{yj}, k_{xj}, k_{yj}, k_{\theta j}$ denote the j-th story mass, the j-th story mass moment of inertia, the eccentricity of the center of stiffness from the center of mass for each axis in j-th story, the x-directional and y-directional story stiffnesses of the j-th story, the torsional stiffness of the j-th story around the center of mass, respectively. ψ denotes the angle of incidence of the earthquake ground motion $\ddot{u}_g$ to the building model.

The following assumptions on the building model are introduced.

- The building model has the stiffness symmetricity with respect to the x-axis and y-axis and exhibits a torsional response under uni-directional earthquake ground motion input (this input does not include rotational motions).
- The center of mass in each story exists in the common vertical line.
- The building model is linearly elastic and has a stiffness-proportional damping matrix.
- The floor is rigid in its in-plane deformation and torsional stiffness of the members are not considered.

In the identification, the following three conditions are used.

1) The first-order modes in the x- and y-direction are known.
2) The floor masses, the locations of the center of mass and stiffness at all the floors are known.
3) The x- and y-directional accelerations at the stiff-side and the flexible-side of all the floors and that on the ground floor are measured.

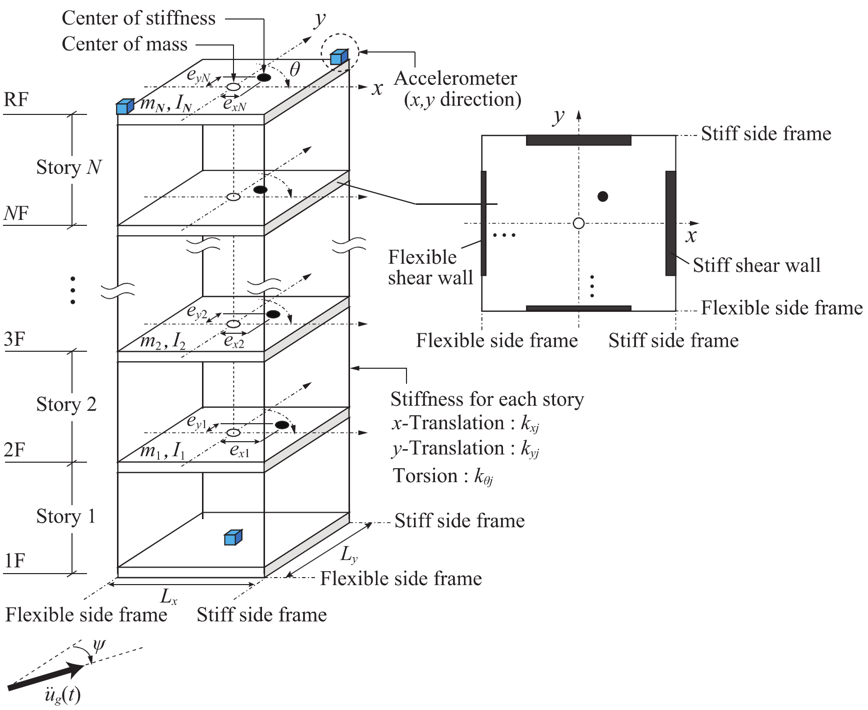

Figure 1 Three-dimensional multi-story building structure model with stiffness eccentricity subjected to uni-directional earthquake ground motion and allocation of accelerometers

3. Identification algorithm

3.1 Identification theory and formulation

The equations of motion of this building model subjected to the earthquake ground acceleration $\ddot{u}_g(t)$ when the angle of incidence is ψ may be expressed by

$$\mathbf{M}\ddot{\mathbf{u}}(t)+\mathbf{C}\dot{\mathbf{u}}(t)+\mathbf{K}\mathbf{u}(t)=-\mathbf{M}\mathbf{r}\ddot{u}_g(t) \tag{1}$$

where the mass, stiffness and damping matrices $\mathbf{M},\mathbf{K},\mathbf{C}$, the displacement vector $\mathbf{u}(t)$ (the *x*, *y*-directional displacements of the center of mass and floor rotation angles $\boldsymbol{\theta}(t)$) and the influence coefficient vector $\mathbf{r}$ may be given as follows.

$$\mathbf{M}=\begin{bmatrix}\mathbf{m}&0&0\\0&\mathbf{m}&0\\0&0&\mathbf{I}\end{bmatrix},\ \mathbf{K}=\begin{bmatrix}\mathbf{K}_{xx}&0&\mathbf{K}_{x\theta}\\0&\mathbf{K}_{yy}&\mathbf{K}_{y\theta}\\\mathbf{K}_{\theta x}&\mathbf{K}_{\theta y}&\mathbf{K}_{\theta\theta}\end{bmatrix},\ \mathbf{C}=\frac{2h_1}{\omega_1}\mathbf{K},\ \mathbf{u}(t)=\begin{Bmatrix}\mathbf{x}(t)\\\mathbf{y}(t)\\\boldsymbol{\theta}(t)\end{Bmatrix},\ \mathbf{r}=\begin{Bmatrix}\mathbf{s}\\\mathbf{c}\\0\end{Bmatrix} \tag{2a-e}$$

ω_1 and h_1 denote the fundamental natural circular frequency and the lowest-mode damping ratio. Other parameters may be defined as follows.

$$\mathbf{m}=\mathrm{diag}\{m_1,m_2,\cdots,m_N\},\ \mathbf{I}=\mathrm{diag}\{I_1,I_2,\cdots,I_N\} \tag{3a,b}$$

$$\mathbf{x}(t)=\{x_1(t),x_2(t),\cdots,x_N(t)\}^T,\ \mathbf{y}(t)=\{y_1(t),y_2(t),\cdots,y_N(t)\}^T,\ \boldsymbol{\theta}(t)=\{\theta_1(t),\theta_2(t),\cdots,\theta_N(t)\}^T \tag{3c-e}$$

$$\mathbf{s}=\{\sin\psi,\sin\psi,\cdots,\sin\psi\}^T,\ \mathbf{c}=\{\cos\psi,\cos\psi,\cdots,\cos\psi\}^T \tag{3f,g}$$

$$\mathbf{K}_{xx}=\begin{bmatrix}k_{x1}+k_{x2}&-k_{x2}&\cdots&0\\-k_{x2}&k_{x2}+k_{x3}&&\vdots\\\vdots&&\ddots&-k_{xN}\\0&\cdots&-k_{xN}&k_{xN}\end{bmatrix},\ \mathbf{K}_{yy}=\begin{bmatrix}k_{y1}+k_{y2}&-k_{y2}&\cdots&0\\-k_{y2}&k_{y2}+k_{y3}&&\vdots\\\vdots&&\ddots&-k_{yN}\\0&\cdots&-k_{yN}&k_{yN}\end{bmatrix} \tag{3h,i}$$

$$\mathbf{K}_{\theta\theta}=\begin{bmatrix}k_{\theta1}+k_{\theta2}&-k_{\theta2}&\cdots&0\\-k_{\theta2}&k_{\theta2}+k_{\theta3}&&\vdots\\\vdots&&\ddots&-k_{\theta N}\\0&\cdots&-k_{\theta N}&k_{\theta N}\end{bmatrix} \tag{3j}$$

$$\mathbf{K}_{x\theta}=\mathbf{K}_{\theta x}^T=\begin{bmatrix}k_{x1}e_{y1}+k_{x2}e_{y2}&-k_{x2}e_{y2}&\cdots&0\\-k_{x2}e_{y2}&k_{x2}e_{y2}+k_{x3}e_{y3}&&\vdots\\\vdots&&\ddots&-k_{xN}e_{yN}\\0&\cdots&-k_{xN}e_{yN}&k_{xN}e_{yN}\end{bmatrix} \tag{3k}$$

$$\mathbf{K}_{y\theta} = \mathbf{K}_{\theta y}^{T} = \begin{bmatrix} -(k_{y1}e_{x1} + k_{y2}e_{x2}) & k_{y2}e_{x2} & \cdots & 0 \\ k_{y2}e_{x2} & -(k_{y2}e_{x2} + k_{y3}e_{x3}) & & \vdots \\ \vdots & & \ddots & k_{yN}e_{xN} \\ 0 & \cdots & k_{yN}e_{xN} & -k_{yN}e_{xN} \end{bmatrix} \tag{3l}$$

The Fourier transformation of Eq.(1) leads to the following equations of motion in the frequency domain.

$$\left(-\omega^2\mathbf{M} + i\omega\mathbf{C} + \mathbf{K}\right)\ddot{\mathbf{U}}(\omega) = \omega^2\mathbf{Mr}\ddot{U}_g(\omega) \tag{4}$$

where $\ddot{\mathbf{U}}(\omega) = \{\ddot{\mathbf{X}}(\omega)^T \ \ddot{\mathbf{Y}}(\omega)^T \ \ddot{\mathbf{\Theta}}(\omega)^T\}^T$ and $\ddot{U}_g(\omega)$ are the Fourier transforms of $\ddot{\mathbf{u}}(t)$ and $\ddot{u}_g(t)$. $\ddot{\mathbf{X}}(\omega)$ and $\ddot{\mathbf{Y}}(\omega)$ are those of $\ddot{\mathbf{x}}(t)$ and $\ddot{\mathbf{y}}(t)$. Unless otherwise noted, The capital letters indicate the Fourier transforms of variables in the time domain and $(\omega),(t)$ are omitted. The x- and y-directional equilibrium of the free-body above the j-th story may be expressed in the frequency domain by

$$\begin{aligned} \omega^2\sum_{k=j}^{N} m_k(\ddot{X}_k + \ddot{X}_g) &= \left(k_{xj} + i\omega\frac{2h_1}{\omega_1}k_{xj}\right)\left\{(\ddot{X}_j - \ddot{X}_{j-1}) + e_{yj}(\ddot{\Theta}_j - \ddot{\Theta}_{j-1})\right\} \\ &= (k_{xj} + i\omega c_{xj})\left\{(\ddot{X}_j - \ddot{X}_{j-1}) + e_{yj}(\ddot{\Theta}_j - \ddot{\Theta}_{j-1})\right\} \end{aligned} \tag{5a}$$

$$\begin{aligned} \omega^2\sum_{k=j}^{N} m_k(\ddot{Y}_k + \ddot{Y}_g) &= \left(k_{yj} + i\omega\frac{2h_1}{\omega_1}k_{yj}\right)\left\{(\ddot{Y}_j - \ddot{Y}_{j-1}) - e_{xj}(\ddot{\Theta}_j - \ddot{\Theta}_{j-1})\right\} \\ &= (k_{yj} + i\omega c_{yj})\left\{(\ddot{Y}_j - \ddot{Y}_{j-1}) - e_{xj}(\ddot{\Theta}_j - \ddot{\Theta}_{j-1})\right\} \end{aligned} \tag{5b}$$

where, $\ddot{X}_0 = 0$, $\ddot{Y}_0 = 0$, $\ddot{\Theta}_0 = 0$ and the viscous damping coefficient c_{xj}, c_{yj} in the j-th story is given by

$$c_{xj} = \frac{2h_1}{\omega_1}k_{xj}, \quad c_{yj} = \frac{2h_1}{\omega_1}k_{yj} \tag{6a,b}$$

Rearrangement of Eqs.(5a) and (5b) with respect to k_{xj}, k_{yj} and c_{xj}, c_{yj} yields

$$k_{xj} + i\omega c_{xj} = \frac{\omega^2\sum_{k=j}^{N} m_k(\ddot{X}_k + \ddot{X}_g)}{(\ddot{X}_j - \ddot{X}_{j-1}) + e_{yj}(\ddot{\Theta}_j - \ddot{\Theta}_{j-1})} \tag{7a}$$

$$k_{yj} + i\omega c_{yj} = \frac{\omega^2\sum_{k=j}^{N} m_k(\ddot{Y}_k + \ddot{Y}_g)}{(\ddot{Y}_j - \ddot{Y}_{j-1}) - e_{xj}(\ddot{\Theta}_j - \ddot{\Theta}_{j-1})} \tag{7b}$$

The lateral stiffnesses k_{xj} and k_{yj} are expressed by the real part of Eqs.(7a) and (7b). In this paper, the building model is linearly elastic. Therefore, Eqs.(7a) and (7b) mean that, if the true physical parameters m_j, e_{xj}, e_{yj} and the true accelerations $\ddot{x}_j, \ddot{y}_j, \ddot{\theta}_j, \ddot{x}_g, \ddot{y}_g$ are given, k_{xj} and k_{yj} (the real part of Eqs.(7a) and (7b)) become constant with respect to frequency.

When k_{xj} and k_{yj} are identified, the information of all frequency bands is not required and it may be better to use the information of high signal/noise (SN) ratio such as the first mode in the x- and y-direction. Ordinarily, the first-mode responses in the x-direction and the y-direction are the dominant component in the responses of building structures. Based on this discussion, some assumptions are introduced as follows.

$$\ddot{X}_j(\tilde{\omega}_{X1}) \approx \ddot{X}_{X1,j}(\tilde{\omega}_{X1}),\ \ddot{Y}_j(\tilde{\omega}_{Y1}) \approx \ddot{Y}_{Y1,j}(\tilde{\omega}_{Y1}),\ \ddot{\Theta}_j(\tilde{\omega}_{X1}) \approx \ddot{\Theta}_{X1,j}(\tilde{\omega}_{X1}),\ \ddot{\Theta}_j(\tilde{\omega}_{Y1}) \approx \ddot{\Theta}_{Y1,j}(\tilde{\omega}_{Y1}) \tag{8a-d}$$

where, $\tilde{\omega}_{X1}, \tilde{\omega}_{Y1}$ denote the frequency bands around the x and y directional first-order frequencies. $\ddot{X}_{X1,j}, \ddot{Y}_{Y1,j}$ are the Fourier transforms of the j-th relative horizontal accelerations $\ddot{x}_{X1,j}, \ddot{y}_{Y1,j}$ at the center of mass in the x- and y- directional first-order modes and $\ddot{\Theta}_{X1,j}, \ddot{\Theta}_{Y1,j}$ are the Fourier transforms of the j-th relative rotational accelerations $\ddot{\theta}_{X1,j}, \ddot{\theta}_{Y1,j}$ in those. Eqs.(8a-d) means that $\tilde{\omega}_{X1}, \tilde{\omega}_{Y1}$ components of acceleration responses $\ddot{x}_j, \ddot{y}_j, \ddot{\theta}_j$ are approximated by the $\tilde{\omega}_{X1}, \tilde{\omega}_{Y1}$ components of the x- and y- directional first-order modal responses $\ddot{x}_{X1,j}, \ddot{y}_{Y1,j}, \ddot{\theta}_{X1,j}, \ddot{\theta}_{Y1,j}$. Substitution of Eqs.(8a-d) into Eqs.(7a) and (7b) provide

$$k_{xj} + i\tilde{\omega}_{X1}c_{xj} \approx \frac{\omega^2 \sum_{k=j}^{N} m_k (\ddot{X}_{X1,k}(\tilde{\omega}_{X1}) + \ddot{X}_g(\tilde{\omega}_{X1}))}{(\ddot{X}_{X1,j}(\tilde{\omega}_{X1}) - \ddot{X}_{X1,j-1}(\tilde{\omega}_{X1})) + e_{yj}(\ddot{\Theta}_{X1,j}(\tilde{\omega}_{X1}) - \ddot{\Theta}_{X1,j-1}(\tilde{\omega}_{X1}))} \tag{9a}$$

$$k_{yj} + i\tilde{\omega}_{Y1}c_{yj} \approx \frac{\omega^2 \sum_{k=j}^{N} m_k (\ddot{Y}_{Y1,k}(\tilde{\omega}_{Y1}) + \ddot{Y}_g(\tilde{\omega}_{Y1}))}{(\ddot{Y}_{Y1,j}(\tilde{\omega}_{Y1}) - \ddot{Y}_{Y1,j-1}(\tilde{\omega}_{Y1})) - e_{xj}(\ddot{\Theta}_{Y1,j}(\tilde{\omega}_{Y1}) - \ddot{\Theta}_{Y1,j-1}(\tilde{\omega}_{Y1}))} \tag{9b}$$

Eqs.(9a) and (9b) will be called “the lateral identification function” and used for identification of k_{xj} and k_{yj}.

The x- and y-directional first-order modal responses $\ddot{x}_{X1,j}, \ddot{y}_{Y1,j}, \ddot{\theta}_{X1,j}, \ddot{\theta}_{Y1,j}$ are required for identification of k_{xj} and k_{yj}. The estimation of modal responses has four proecsses. In the first process, the transfer function from ground acceleration to N-th relative horizontal accelerations at the stiff-side and flexible-side are processed by Tukey window. In the second process, the filter-processed transfer functions are processed by IFFT and the x- and y-directional first-order modal responses at the stiff- and flexible-side on the top floor are calculated. In the third process, these responses are multiplied by the x- and y-directional first-order mode shapes at the stiff- and flexible-side and the x- and y-directional first-order modal responses $\ddot{x}_{X1,Sj}, \ddot{x}_{X1,Fj}, \ddot{y}_{Y1,Sj}, \ddot{y}_{Y1,Fj}$ at each side on each floor are calculated. In the last process, $\ddot{x}_{X1,j}, \ddot{y}_{Y1,j}$ are calculated by linear interpolation from $\ddot{x}_{X1,Sj}, \ddot{x}_{X1,Fj}, \ddot{y}_{Y1,Sj}, \ddot{y}_{Y1,Fj}$ and $\ddot{\theta}_{X1,j}, \ddot{\theta}_{Y1,j}$ are calculated to divide the differences of the modal responses at each side by floor sizes. In this paper, It is assumed that the center of mass exists at the center of floor and $\ddot{x}_{X1,j}, \ddot{y}_{Y1,j}, \ddot{\theta}_{X1,j}, \ddot{\theta}_{Y1,j}$ are calculated by

$$\ddot{x}_{X1,j} = \frac{\ddot{x}_{X1,Fj} + \ddot{x}_{X1,Sj}}{2},\ \ddot{y}_{Y1,j} = \frac{\ddot{y}_{Y1,Fj} + \ddot{y}_{Y1,Sj}}{2},\ \ddot{\theta}_{X1,j} = \frac{\ddot{x}_{X1,Sj} - \ddot{x}_{X1,Fj}}{L_y},\ \ddot{\theta}_{Y1,j} = \frac{\ddot{y}_{Y1,Fj} - \ddot{y}_{Y1,Sj}}{L_x} \tag{10a-d}$$

3.2 Calculation procedure of identification value of lateral stiffness

The calculation procedure of identification value of lateral stiffness can be summarized as follows. Fig.2 shows the explanation of Steps 1-3.

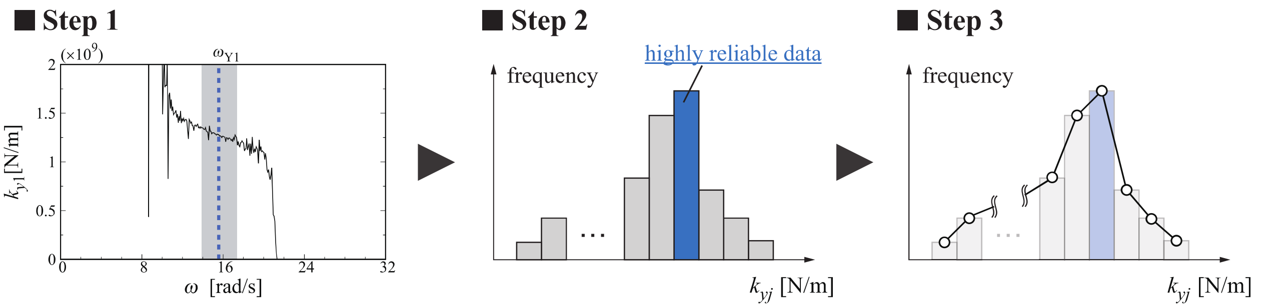

Figure 2 Identification procedure in frequency domain (Steps 1-3)

(Step 1) Focusing on the x and y directional first-order circular frequencies, pick up n data points from the identification results derived by using "the lateral identification function". $\tilde{\omega}_{X1}$ is used for identification of k_{xj} and $\tilde{\omega}_{Y1}$ is used for that of k_{yj} . Then, histograms are calculated from the N data points.

(Step 2) The class indicating the maximum frequency may be highly reliable class in histogram and the average of the data classified this class is calculated.

(Step 3) Compute the coefficient of variation by considering the average as the sample mean.

(Step 4) Vary the sample number n and repeat Steps 1-3.

(Step 5) Find the value corresponding to the smallest coefficient of variation and regard that value as the identification value of lateral stiffness.

The range width per class (upper and lower limits of each class) can be determined by using the number of classes and this can also be defined from the Sturges' rule by

$$\text{Number of classes} = 1 + \log_2 n \tag{11}$$

In this paper, the sample number n is varied from 30 to 100.

4. Verification of accuracy of the proposed method using numerical investigation

4.1 Analysis condition

To investigate the accuracy of the proposed identification method, the numerical analysis data, the accelerations at the stiff-side and flexible-side on the top floor and the input earthquake ground motion, are used as substitutes of measured data. It is assumed that the x- and y-directional first-order mode shapes are already known.

Table 1 and Table 2 show the physical properties and eigenvalue of analysis models, respectively. The object building models are five-story shear models with bi-axial eccentricity and two models (BS-model and BC-model) are considered. BS-model and BC-model are considered as the models the eigenvalue of the translation mode of which are separated from and close to the eigenvalue of the torsional mode. The 1th, 2nd and 3rd mode of both BS-model and BC-model are the y-lateral mode, the x-lateral mode and the torsional mode, respectively. The height distribution of the story stiffness is defined so that fundamental natural period of the model without eccentricity is 0.4 s and the lowest mode is a straight line for the model without eccentricity. The stiffness-proportional damping matrix is assumed and the lowest-mode damping ratio is 0.03. The responses of the models are calculated by using Newmark-beta method with β=1/4 (constant acceleration method) and El Centro 1940 NS is used as the input earthquake ground motion. The maximum-

Table 1 Physical properties of torsionally coupled building

Model	Floor	L_x	L_y	m	I	e_x	e_y	Story	k_x	k_y	k_θ	R_{ex}	R_{ey}
		[m]	[m]	[kg]	[kg·m^2]	[m]	[m]		[N/m]	[N/m]	[N·m/rad]	-	-
BS-model	2	24	12	3.46×10^5	2.07×10^7	1.80	1.20	1	1.41×10^9	1.28×10^9	1.66×10^{11}	0.112	0.160
	3					1.80	1.20	2	1.31×10^9	1.19×10^9	1.55×10^{11}	0.112	0.160
	4					1.99	1.20	3	1.13×10^9	1.02×10^9	1.88×10^{11}	0.0939	0.148
	5					1.99	1.20	4	8.44×10^8	7.67×10^8	1.41×10^{11}	0.0939	0.148
	R					1.99	1.20	5	4.69×10^8	4.26×10^8	7.83×10^{10}	0.0939	0.148
BC-model	2	24	12	3.46×10^5	2.07×10^7	1.20	0.60	1	1.66×10^9	1.28×10^9	1.06×10^{11}	0.133	0.0758
	3					1.20	0.60	2	1.55×10^9	1.19×10^9	9.88×10^{10}	0.133	0.0758
	4					1.00	0.60	3	1.33×10^9	1.02×10^9	8.47×10^{10}	0.110	0.0756
	5					1.00	0.60	4	9.98×10^8	7.67×10^8	6.35×10^{10}	0.110	0.0756
	R					1.00	0.60	5	5.54×10^8	4.26×10^8	3.53×10^{10}	0.110	0.0756

Table 2 Eigenvalue analysis of torsionally coupled building (number in parenthesis: natural frequency [Hz])

Property	BS-model			BC-model		
	1st	2nd	3rd	1st	2nd	3rd
Natural circular frequency [rad/s]	15.4 (2.45)	16.4 (2.61)	25.1 (3.99)	15.3 (2.44)	17.6 (2.80)	19.1 (3.04)
Natural period [s]	0.409	0.384	0.250	0.411	0.358	0.329
Damping ratio [%]	3.00	3.20	4.90	3.00	3.44	3.74
Participation factor [-]	-3.07×10^{-2}	0.224	-5.00×10^{-4}	-1.57×10^{-2}	0.188	2.07×10^{-2}

acceleration is also normalized to be 20 gal and the angle of incidence of the earthquake ground motion to building models is 45 degree angle ($\psi = 1/4\pi$).

To take into account the influence of measurement noise level on the accuracy of identification, the data generated by using the following equation are used.

$$\text{Noise level} = \frac{\text{RMS value of band limited white noise}}{\text{RMS value of signal without noise}} \tag{12}$$

Noise-free data and data with 5% and 10% noise are used for identification. The band-limited white noise is added to the response analysis results and the input ground motions.

4.2 Identification of lateral stiffness

Fig.3 and Fig.4 show the real part of the x-directional lateral identification functions defined in Eqs.(9a) in the first story for BS-model and BC-model. In Fig.3a and Fig.4a, identification results calculated by using Eqs.(7a) are also shown. The red lines indicate the true values of each model.

When Eqs.(7a) is used for identification and the noise is free, It can be observed that the results exhibit almost constant distributions in a wide frequency range. This indicates that Eqs.(7a) is theoretically valid. On the other hand, When Eqs.(9a) is used, the results totally do not exhibit horizontal constant distributions. However, the results are stable at the x-directional first-order circular frequency and correspond well with the true values of each model. If the y-directional lateral stiffness are identified, it is confirmed that the results are stable at the y-directional first-order circular frequency and correspond well the true values of each model. There is the same tendency in other noise levels and that has been confirmed also in other stories.

Fig.5 and Fig.6 show the identified values of lateral stiffness in each story for BS-model and BC-model without and with noise. The values of horizontal axis indicate ratios of the identified values to the true

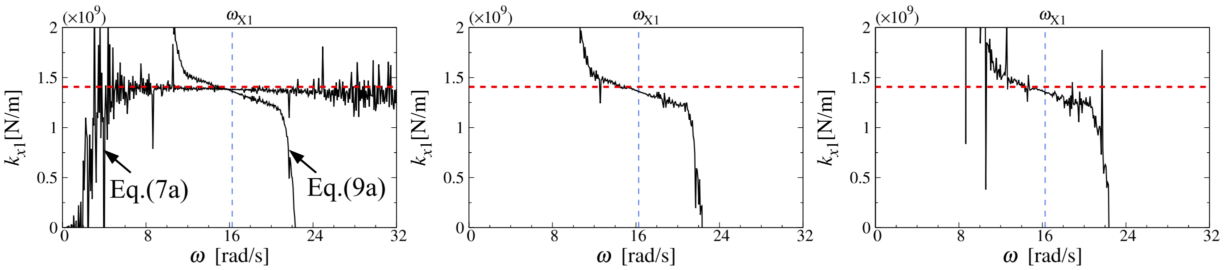

(a) noise level 0% (b) noise level 5% (c) noise level 10%

Figure 3 Identification result of x-directional lateral stiffness in the first story (BS-model)

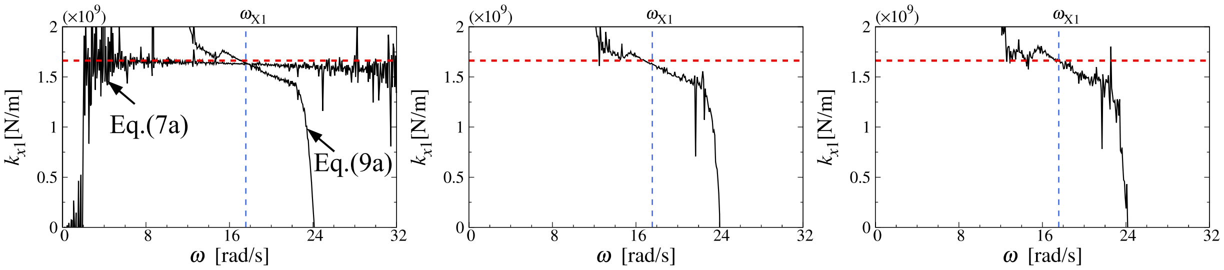

(a) noise level 0% (b) noise level 5% (c) noise level 10%

Figure 4 Identification result of x-directional lateral stiffness in the first story (BC-model)

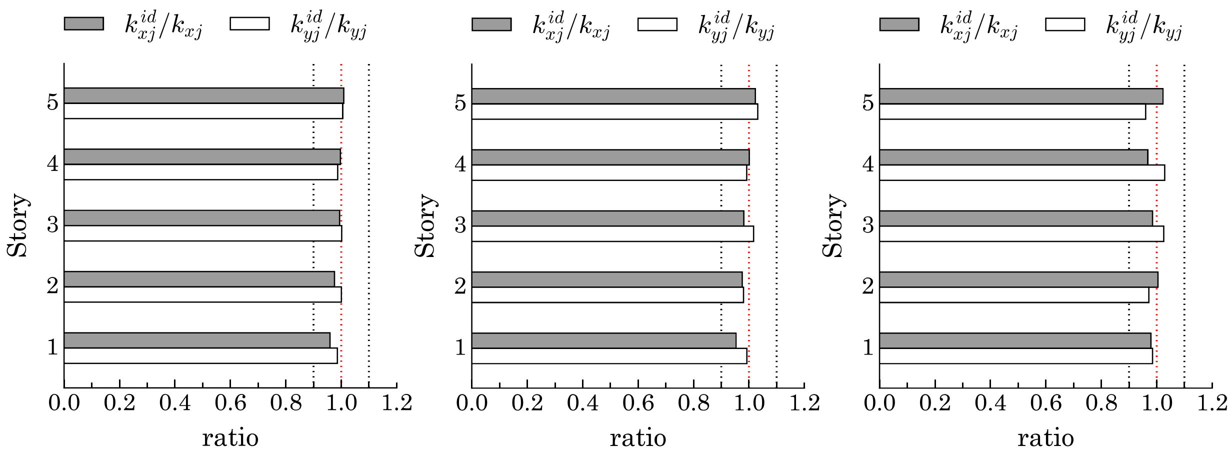

(a) noise level 0% (b) noise level 5% (c) noise level 10%

Figure 5 Identified vale of lateral stiffnesses in each story (BS-model)

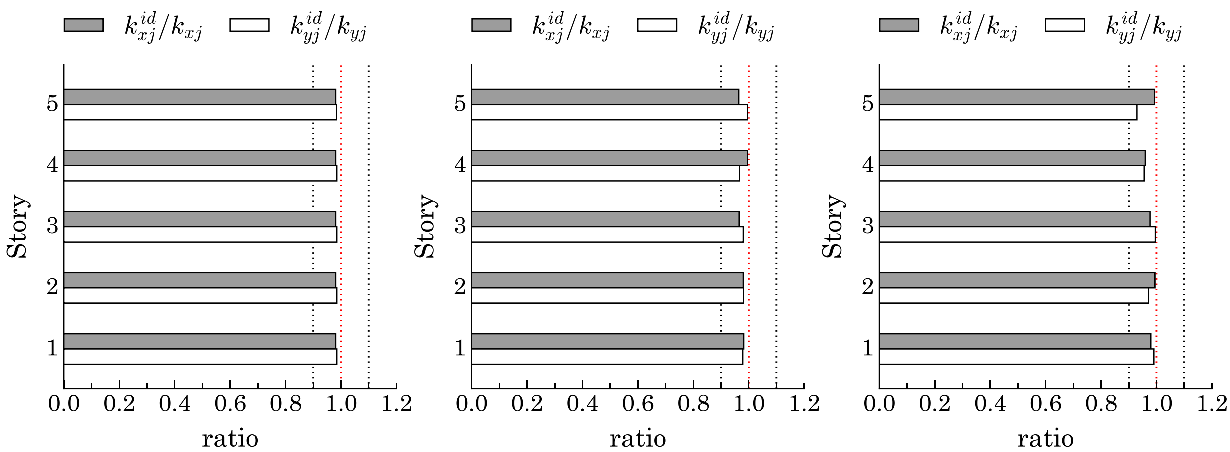

(a) noise level 0% (b) noise level 5% (c) noise level 10%

Figure 6 Identified vale of lateral stiffnesses in each story (BC-model) values. It can be found that the errors are within 9% for all the noise levels. Therefore, it may be concluded that the proposed method possesses an acceptable accuracy.

5. Conclusion

A new method of frequency-domain physical-parameter SI has been developed for three-dimensional building structures with stiffness eccentricity. The conclusions may be summarized as follows.

1) The dynamic equilibrium of the free body above the *j*-th story can be used to identify the *j*-th two-directional story stiffnesses. It is required to measure the horizontal accelerations at stiff-side and flexible-side on the top floor to identify the story stiffnesses. Compared to the previous approach, the identification algorithm is very simple and avoid complicated mathematical manipulation. Therefore, it provides good usability. In addition, it is not required to measure horizontal accelerations at all floors. Furthermore, the data with high SN ratio, which is picked up based on low-order modal information, is used for the identification and this makes the proposed method robust for noise. The two-directional story stiffnesses for each story can be identified independently and the identified value does not affect those of other stories. However, it should be noted that the *x*- and *y*-directional first-order mode shapes are necessary for identification.
2) Numerical investigation demonstrated that the proposed identification method possesses an acceptable accuracy. Even if the data with the noise is used for identification, the identification results are quite stable around the low-order natural frequency and are robust for noise. However, it should be noted that this conclusion is obtained under restrictive conditions.

6. Acknowledgements

KN formulated the problem, conducted the computation, and wrote the paper.

7. References

[1] Hart, G.C. and Yao, J.T.P. (1977): System identification in structural dynamics, *J. Engng. Mech. Div.*, ASCE, 103, 1089-1104.

[2] Agbabian, M.S, Masri, S.F., Miller, R.K. and Caughey, T.K. (1991): System identification approach to detection of structural changes, *J. Engng. Mech.*, ASCE, 117, 370-390.

[3] Nagarajaiah, S. and Basu, B. (2009): Output only modal identification and structural damage detection using time frequency & wavelet techniques, *Earthquake Eng. and Eng. Vib.*, 8, 583-605.

[4] Suzuki, Y., Adachi, N., Nozawa, T., Ikeura, T. and Kusaka, A. (2010): Prediction of artificial seismic damage of an actual building at a steel beam based on forced vibration test and microtremor, *J. Technol., Architectural Inst. of Japan*, 33, 473-478 (in japanese).

[5] Shiraishi, M., Morii, T. and Mita, A. (2015): Verification of local damage detection method based on forced vibration test of 5 story RC building with artificial seismic damages, *J. Structural and Construction Eng., Architectural Inst. of Japan*, 711, 745-755 (in Japanese).

[6] Nakamura, M. and Yasui, Y. (1999): Damage evaluation of a steel structure subjected to strong earthquake motion based on ambient vibration measurements, *J. Structural and Construction Eng., Architectural Inst. of Japan*, 517, 61-68 (in Japanese).

[7] Takewaki, I. and Nakamura, M. (2000): Stiffness-damping simultaneous identification using limited earthquake records, *Earth. Eng. Struct. Dyn.*, 29(8), 1219-1238.

[8] Udwadia, F.E., Sharma, D.K. and Shah, P.C. (1978): Uniqueness of damping and stiffness distributions in the identification of soil and structural systems, *J. Applied Mech.*, ASME, 45, 181-187.

[9] Takewaki, I. and Nakamura, M. (2005): Stiffness-damping simultaneous identification under limited observation, *J. Eng. Mech.*, ASCE, 131, 1027-1035.

[10] Takewaki, I. and Nakamura, M. (2010): Temporal variation of modal properties of a base-isolated building during an earthquake, *Journal of Zhejiang University-SCIENCE A*, 11, 1-8.

[11] Ikeda, A., Fujita, K. and Takewaki, I. (2014): Story-wise system identification of actual shear building using ambient vibration data and ARX model, *Earthquakes and structures*, 7, 1093-1118.

[12] Ikeda, A., Fujita, K. and Takewaki, I. (2015): Reliability of system identification technique in super high-rise building, *Frontiers in Built Environment*, 1: 11.

[13] Fujita, K., Ikeda, A. and Takewaki, I. (2015): Application of story-wise shear building identification method to actual ambient vibration, *Frontiers in Built Environment*, 1: 2.

[14] Maeda, T., Yoshitomi, S. and Takewaki, I. (2011): Stiffness-damping identification of buildings using limited earthquake records and ARX model, *J. Struct. Construction Eng., Architectural Inst. of Japan*, 666, 1415-1423 (in Japanese).

[15] Kuwabara, M., Yoshitomi, S. and Takewaki I. (2013): A new approach to system identification and damage detection of high-rise buildings, *Struct. Control Health Monitoring*, 20, 703-727.

[16] Minami, Y., Yoshitomi, S. and Takewaki, I. (2013): System identification of super high-rise buildings using limited vibration data during the 2011 Tohoku (Japan) earthquake, *Struct. Control Health Monitoring*, 20, 1317-1338.

[17] Ikeda, Y. and Hanafusa, H. (2014): Direct identification of stiffness for flexural-shear building model based on earthquake observation, *J. Struct. Construction Eng., Architectural Inst. of Japan*, 705, 1601-1611 (in Japanese).

[18] Shintani, K., Yoshitomi, S. and Takewaki, I. (2017): Direct linear system identification method for multi-story three-dimensional building structure with general eccentricity, *Frontiers in Built Environment*, 3: 17.

